# Kinetics and Thermodynamics of Redox Processes in Room Temperature Ionic Liquids: The Use of Voltammetry and the Disproportionation of Radical Cations of *N*,*N*-Dimethyl-*p*-phenylenediamine in 1-Butyl-3-methylimidazolium Tetrafluoroborate

**Edward O. Barnes, Aoife M. O'Mahony, Stephen R. Belding, and Richard G. Compton***

Department of Chemistry, Physical and Theoretical Chemistry Laboratory, Oxford University, South Parks Road, Oxford, OX1 3QZ, United Kingdom

The voltammetry of *N*,*N*-dimethyl-*p*-phenylenediamine, DMPD, in the room temperature ionic liquid (RTIL) 1-butyl-3-methylimidazolium tetrafluoroborate, $[C_4mim][BF_4]$ is studied by means of microdisc voltammetry over a wide range of voltage scan rates incorporating the transition from linear to convergent diffusion. Two voltammetric waves were recorded corresponding to the formation of the radical cation $DMPD^+$ and dication $DMPD^{2+}$; both are stable on the voltammetric time scale. Double potential step chronoamperometry was used to measure the diffusion coefficients of DMPD and $DMPD^+$. These values, in conjunction with simulations of the cyclic voltammetry, permit the inference of the equilibrium constant and kinetics for the comproportionation of DMPD and $DMPD^{2+}$ forming $DMPD^+$ to be studied.

## 1. Introduction

Room temperature ionic liquids (RTILs) have led to substantial synthetic innovations in both academic[1−3] and industrial[4] contexts. Advantages such as solvent tunability,[5] greenness,[6] recyclability, and negligible volatility are seen over conventional nonaqueous solvents. However, unlike reactions in the latter media, the measurement of reaction parameters, both kinetic and thermodynamic, has lagged, and comparatively less data is available to guide the planning and interpretation of chemistry in the RTIL environment.

Voltammetry, at least in principle, offers an experimentally simple yet accurate route into the quantitative measurement of both kinetic and thermodynamic data. For example, in the case of an arbitrary species, A, which can undergo oxidation to species B and C:

$$A - e^- \rightleftharpoons B(E^{\ominus}_{f,A/B}) \quad (1)$$

$$B - e^- \rightleftharpoons C(E^{\ominus}_{f,B/C}) \quad (2)$$

If two separate voltammetric features are attributable to these processes, then their analysis can give information about the comproportionation reaction:[7]

$$A + C \rightleftharpoons 2B \quad (3)$$

where, specifically, the formal potentials $E^{\Theta}_{f,A/B}$ and $E^{\Theta}_{f,B/C}$ will provide information about the equilibrium constant:

$$K_{eqm} = \frac{[B]^2}{[A][C]} \quad (4)$$

and $\Delta G^{\Theta}$ for reaction 3:

$$\Delta G^{\ominus} = -RT\ln(K_{eqm}) = -F(E^{\ominus}_{f,B/C} - E^{\ominus}_{f,A/B}) \quad (5)$$

The kinetics of reaction 3 may sometimes be discernible from the precise voltammetric waveshapes and their separation.[8] However, in the context of voltammetry using large planar electrodes ("macroelectrodes"), Savéant and Andrieux have shown in a paper, long regarded as a classic,[9] that if species A, B, and C have identical diffusion coefficients, $D_A$, $D_B$, and $D_C$, then the voltammetry is completely insensitive to the rate of comproportionation. The same is true of voltammetry recorded under diffusional modes other than linear.[7] Only if there is an appreciable disparity in the diffusion coefficients can the kinetics of reaction 3 become apparent in the voltammetry. Accordingly, voltammetry has been relatively little used in the context of measuring comproportionation kinetics except insofar that it has been coupled to spectroscopic methods, such as electron spin resonance (ESR)[9] and UV−visible spectroscopy.[10] At the heart of this neglect is the fact that, in most aqueous and nonaqueous systems, species A, B, and C often have closely similar diffusion coefficients unless they are structurally very dissimilar.

As electrochemical research using RTILs as solvents[11−17] has matured, it has become apparent that, unlike conventional solvents such as DMF, DMSO, and acetonitrile, the difference in diffusion coefficients between structurally similar species in a redox couple is not always insignificant. An extreme example, discovered by Buzzeo et al.,[18] is that of the oxygen/superoxide $(O_2/O_2^-)$ couple in which the anion has a diffusion coefficient about 30 times smaller than the neutral parent in the RTIL *n*-hexyltriethylammonium bis(trifluoromethanesulfonyl)imide $([N_{6222}][N(Tf)_2])$. Work by Evans et al.[12] and by Hapiot et al.[19] have shown that even for aromatic molecules, such as *N*,*N*,*N*′,*N*′-tetramethyl-para-phenylenediamine, the diffusion coefficients differ significantly between the neutral parent and the corresponding radical cation and dication despite close structural similarity. Analyte ions of higher charge typically diffuse less rapidly because of electrostatic interaction with the ions in the solvent. As a consequence, it can be anticipated that, in ionic liquids, voltammetric analysis can be used as a means of obtaining information about the rate of comproportionation in solution.

* Corresponding author. Fax: +44 (0) 1865 275410. Tel.: +44 (0) 1865 275413. E-mail: richard.compton@chem.ox.ac.uk.

10.1021/je900770b 
Published on Web 11/12/2009

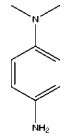

**Figure 1.** Structure of *N*,*N*-dimethyl-*p*-phenylenediamine (DMPD).

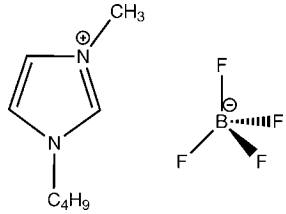

**Figure 2.** Structure of the ionic liquid 1-butyl-3-methylimidazolium tetrafluoroborate ([$C_4$mim][$BF_4$]).

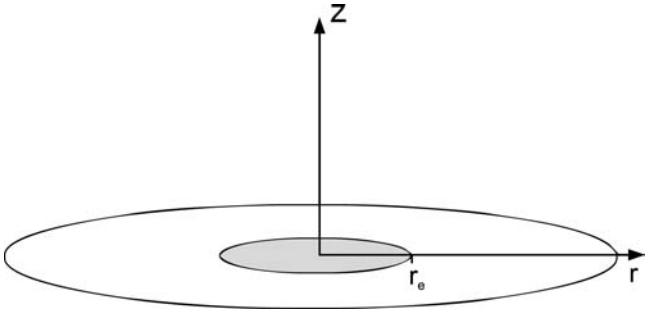


**Figure 3.** Circular disk electrode inlaid on an insulating support.

In this paper we consider the oxidation of *N*,*N*-dimethyl-*p*-phenylenediamine, DMPD (Figure 1), in the ionic liquid 1-butyl-3-methylimidazolium tetrafluoroborate, [$C_4$mim][$BF_4$] (Figure 2), using a microdisc electrode. It is shown that comparison between experimental and simulated data can be used to extract both kinetic and thermodynamic data, including information about comproportionation. Also noted is the value of double potential step chronoamperometry in elucidating the diffusion coefficients of DMPD and $DMPD^+$.[14]

## 2. Theory

We consider a stepwise two electron oxidation reaction at a microdisc electrode (Figure 3), as defined by eqs 1 and 2, where we additionally allow for comproportionation (eq 3). The heterogeneous rate constants for the first two steps are $k^0_{A/B}$ and $k^0_{B/C}$, respectively. The homogeneous rate constant for comproportionation is $k_{comp}$ and for disproportionation is $k_{disp}$. The equilibrium constant for eq 3 is therefore $K_{eqm} = (k_{comp})/(k_{disp})$. Specifically we consider the case of cyclic voltammetry.

$$\frac{\partial c_A}{\partial t} = D_A\left(\frac{\partial^2 c_A}{\partial r^2} + \frac{1}{r}\frac{\partial c_A}{\partial r} + \frac{\partial^2 c_A}{\partial z^2}\right) + k_{disp}c_B^2 - k_{comp}c_A c_C \quad (6)$$

$$\frac{\partial c_B}{\partial t} = D_B\left(\frac{\partial^2 c_B}{\partial r^2} + \frac{1}{r}\frac{\partial c_B}{\partial r} + \frac{\partial^2 c_B}{\partial z^2}\right) - 2(k_{disp}c_B^2 - k_{comp}c_A c_C) \quad (7)$$

$$\frac{\partial c_C}{\partial t} = D_C\left(\frac{\partial^2 c_C}{\partial r^2} + \frac{1}{r}\frac{\partial c_C}{\partial r} + \frac{\partial^2 c_C}{\partial z^2}\right) + k_{disp}c_B^2 - k_{comp}c_A c_C \quad (8)$$

where all symbols are defined in Table 1.

***2.1. Cyclic Voltammetry.*** In the cyclic voltammetry experiment, the applied potential, $E$, is swept from an initial value, $E_i$, to a more oxidizing value, $E_f$, and then back to the initial value. The value of $E$ is therefore calculated at any time on the forward sweep using eq 9 and on the reverse sweep using eq 10, where $\upsilon$ is the voltage scan rate and $t$ is the time:

$$E_{forward} = E_i + \upsilon t \quad (9)$$

$$E_{reverse} = 2E_f + E_i - \upsilon t \quad (10)$$

When $t > 0$, $z = 0$, and $r \le r_e$, the boundary conditions are the Butler−Volmer conditions describing species A and C and conservation of mass for species B:

$$D_A\left(\frac{\partial c_A}{\partial z}\right)_0 = k^0_{A/B}c_{B,0}\exp\left(-\alpha_{A/B}\frac{F(E - E^{\ominus}_{f,A/B})}{RT}\right) - k^0_{A/B}c_{A,0}\exp\left((1 - \alpha_{A/B})\frac{F(E - E^{\ominus}_{f,A/B})}{RT}\right)$$

$$D_B\left(\frac{\partial c_B}{\partial z}\right)_0 = -D_A\left(\frac{\partial c_A}{\partial z}\right)_0 - D_C\left(\frac{\partial c_C}{\partial z}\right)_0$$

$$D_C\left(\frac{\partial c_C}{\partial z}\right)_0 = -k^0_{B/C}c_{C,0}\exp\left(-\alpha_{B/C}\frac{F(E - E^{\ominus}_{f,B/C})}{RT}\right) + k^0_{B/C}c_{B,0}\exp\left((1 - \alpha_{B/C})\frac{F(E - E^{\ominus}_{f,B/C})}{RT}\right)$$

The remaining boundary conditions are:

$t = 0$, all $r$, all $z$

$$c_A = c^*_A \qquad c_B = 0 \qquad c_C = 0$$

$t > 0$, $r > r_e$, $z = 0$

$$\frac{\partial c_A}{\partial z} = 0 \qquad \frac{\partial c_B}{\partial z} = 0 \qquad \frac{\partial c_C}{\partial z} = 0$$

$t > 0$, all $r$, $z \to \infty$

$$\frac{\partial c_A}{\partial z} = 0 \qquad \frac{\partial c_B}{\partial z} = 0 \qquad \frac{\partial c_C}{\partial z} = 0$$

$t > 0$, $r \to \infty$, all $z$

$$\frac{\partial c_A}{\partial r} = 0 \qquad \frac{\partial c_B}{\partial r} = 0 \qquad \frac{\partial c_C}{\partial r} = 0$$

$t > 0$, $r = 0$, all $z$

$$\frac{\partial c_A}{\partial r} = 0 \qquad \frac{\partial c_B}{\partial r} = 0 \qquad \frac{\partial c_C}{\partial r} = 0$$

**Table 1. Dimensional Parameters**

| dimensional parameter | definition |
|---|---|
| $\alpha_{X/Y}$ | transfer coefficient for $X - e^- \rightleftharpoons Y$/unitless |
| $c_X$ | concentration of species X/mol·$m^{-3}$ |
| $c_{X,0}$ | concentration of species X at the electrode surface/mol·$m^{-3}$ |
| $c^*_X$ | concentration of species X in bulk solution/mol·$m^{-3}$ |
| $D_X$ | diffusion coefficient of species X/$m^2$·$s^{-1}$ |
| $E$ | applied potential/V |
| $E^{\ominus}_{f,X/Y}$ | formal reduction potential for $X - e^- \rightleftharpoons Y$/V |
| $k^0_{X/Y}$ | electrochemical rate constant for $X - e^- \rightleftharpoons Y$/m·$s^{-1}$ |
| $k_{comp}$ | rate constant for comproportionation/$dm^3$·$mol^{-1}$·$s^{-1}$ |
| $k_{disp}$ | rate constant for comproportionation/$dm^3$·$mol^{-1}$·$s^{-1}$ |
| $i$ | current/A |
| $j$ | flux across the electrode/mol·$m^2$·$s^{-1}$ |
| $r$ | radial coordinate/m |
| $t$ | time/s |
| $\upsilon$ | scan rate/V·$s^{-1}$ |
| $z$ | axial coordinate/m |

***2.2. Computational Details.*** The problem is generalized by means of a transformation into nondimensional form using a conventional set of normalized parameters (defined in Table 2).

The resulting set of normalized diffusion equations were published by Belding et al.[7] The boundary conditions given in the previous sections are readily formulated in terms of normalized variables using the definitions given in Table 2. The problem is then discretized using the alternating direct implicit method[20,21] (ADI) and solved numerically using the iterative Newton−Raphson scheme.[22] The discretized spatial mesh is analogous to that reported by Gavaghan[23] (Figure 4) and converged to within 0.1 %. Each temporal increment is optimized during run time such that convergence to within 0.01 % is obtained. All programs were written in C++ and compiled using a Borland compiler. The simulations were run on a desktop personal computer with a processor speed of ≈ 3 GHz. Approximately 20 min of central processing unit time were required to simulate a single voltammogram.

## 3. Experimental Section

***3.1. Chemical Reagents.*** 1-Butyl-3-methylimidazolium tetrafluoroborate ([$C_4$mim][$BF_4$]) was kindly donated by Merck KGaA. DMPD (Aldrich, > 97 %), ferrocene (Aldrich, 98 %), tetrabutylammonium perchlorate (TBAP, Fluka, Puriss electrochemical grade, > 99.99 %), and acetonitrile (Fischer Scientific, dried and distilled, > 99.99 %) were used as received without further purification.

***3.2. Instrumental Section.*** Electrochemical experiments were performed using a computer controlled $\mu$-Autolab potentiostat (Eco-Chemie, Netherlands). A conventional two-electrode system was used, typically with a platinum electrode (10 $\mu$m diameter) as the working electrode and a 0.3 mm diameter platinum wire as a quasi-reference electrode. The platinum microdisc working electrode was polished on soft lapping pads (Kemet Ltd., U.K.) using alumina powder (Buehler, IL) of (5.0, 1.0, and 0.3) $\mu$m sizes. The electrode diameter was calibrated electrochemically by analyzing the steady-state voltammetry of a 2 mM solution of ferrocene in acetonitrile containing 0.1 M TBAP, with a diffusion coefficient for ferrocene of $2.3 \cdot 10^{-5}$ $cm^2 \cdot s^{-1}$ at 293 K.[24]

The electrodes were housed in a glass cell "T-cell" designed for investigating microsamples of ionic liquids under a controlled atmosphere[25] (Figure 5). RTILs are sensitive to water,[25,26] and the presence of water can alter the viscosity of the ionic liquid and reduce the electrochemical window; therefore, the samples are purged under vacuum before voltammetry is carried out. In addition, this procedure removes electroactive oxygen from solution.[27] The working electrode was modified with a section of disposable micropipet tip to create a small cavity above the disk into which a drop (20 $\mu$L) of ionic liquid was placed. DMPD was directly dissolved in [$C_4$mim][$BF_4$] at concentration of 20 mM. Prior to voltammetric scanning, the RTIL solution was purged under vacuum (Edwards high vacuum pump, Model ES 50) for about 90 min, which served to remove trace atmospheric moisture naturally present in the RTIL. All experiments were performed inside a fume cupboard, in a thermostatted box (previously described by Evans et al.)[12] which also functioned as a Faraday cage. The temperature was maintained at (298 ± 1.0) K.

**Table 2. Normalized Parameters**

| normalized parameter | definition |
|---|---|
| $J$ | $i/(Fc_A^* D_A r_e)$ |
| $K^0$ | $(k^0 r_e)/D_A$ |
| $K_{comp}$ | $(k_{comp} c_A^* r_e^2)/D_A$ |
| $K_{disp}$ | $(k_{disp} c_A^* r_e^2)/D_A$ |
| $\theta$ | $(F(E - E_{f,A/B}^{\ominus}))/(RT)$ |
| $R$ | $r/r_e$ |
| $\sigma$ | $(r_e^2 F v)/(D_A RT)$ |
| $\tau$ | $(D_A t)/r_e^2$ |
| $x$ | $c_X/c_X^*$ |
| $x_0$ | $c_{X,0}/c_X^*$ |
| $Z$ | $z/r_e$ |

***3.3. Results and Discussion.***

***3.3.1. Chronoamperometry.*** Double potential step chronoamperometric transients at the platinum electrode (10 $\mu$m diameter) were achieved using a sample time of 0.01 s. A solution of approximately 20 mM DMPD in [$C_4$mim][$BF_4$] was pretreated by holding the potential at a point of zero current for 20 s, after which the potential was stepped to a position after the oxidative peak for DMPD corresponding to transport-controlled diffusion, and the current was measured for 5 s. The potential was then stepped to a position after the reductive peak for $DMPD^+$ corresponding to transport-controlled diffusion, and the current response was measured for a further 5 s. To extract diffusion coefficients and solubility data from these transients, the first potential step was fitted using the nonlinear curve-fitting function in the software package Origin 7.0 (Microcal Software, Inc.) according to the following equations proposed by Shoup and Szabo:[28]

$$i = -4nFD_{DMPD}c_{DMPD}r_e f(\tau) \tag{11}$$

$$f(\tau) = 0.7854 + 0.4432\tau^{-1/2} + 0.2146\exp(-0.3912\tau^{-1/2}) \tag{12}$$

$$\tau = \frac{D_{DMPD}t}{r_e^2} \tag{13}$$

where $n$ is the number of electrons transferred, $F$ is the Faraday constant, $D_{DMPD}$ is the diffusion coefficient, $c_{DMPD}$ is the initial concentration of parent species, $r_e$ is the radius of the disk electrode, $t$ is the time, and $f(\tau)$ is a function describing the slope of the transient. The equations used in this approximation are sufficient to give $D_{DMPD}$ and $c_{DMPD}$ within an uncertainty of ± 0.6 %. The value of the parameter $D_{DMPD^+}$ was elucidated by fitting the transient for the second potential step using simulation software developed by Klymenko et al.[14]

The fitted transient is shown in Figure 6 and the corresponding values of $c_{DMPD}$, $D_{DMPD}$, and $D_{DMPD^+}$ recorded in Table 3. It is important to note the value of $c_{DMPD} = 19.5$ mM obtained from fitting the chronoamperometric transient to the Shoup and Szabo equation is in good agreement with the value of $c_{DMPD} \approx 20$ mM used in the experiment. As noted in other situations,[18] despite structural similarity between DMPD and $DMPD^+$, the discrepancy in diffusion coefficients is not insignificant. It is important to note that the potentials applied over the course of the double-step experiment are not sufficient to bring about the transfer of a second electron ($DMPD^+ - e^- \rightleftharpoons DMPD^{2+}$). The concentration of $D_{DMPD^{2+}}$ in solution is negligible, and consequently, comproportionation cannot occur: Figure 6 is independent of the effects of comproportionation regardless of the values of $D_{DMPD}$, $D_{DMPD^+}$, and $D_{DMPD^{2+}}$.

***3.3.2. Cyclic Voltammetry.*** The kinetic and thermodynamic parameters of the two redox couples were elucidated by means of cyclic voltammetry. The oxidation of DMPD was examined in [$C_4$mim][$BF_4$]. Cyclic voltammetry for the oxidation of 20 mM DMPD was carried out on a Pt microelectrode (diameter of 10 $\mu$m) at scan rates ranging from 10 $mV \cdot s^{-1}$ to 1 $V \cdot s^{-1}$. The voltammograms are typically scanned from (0 to 1.5) V versus a Pt quasi-reference electrode. Two oxidation peaks were observed for scan rates of 10 $mV \cdot s^{-1}$ to 1 $V \cdot s^{-1}$, shown in Figure 7 at potentials of (0.4 and 0.9) V. These correspond,

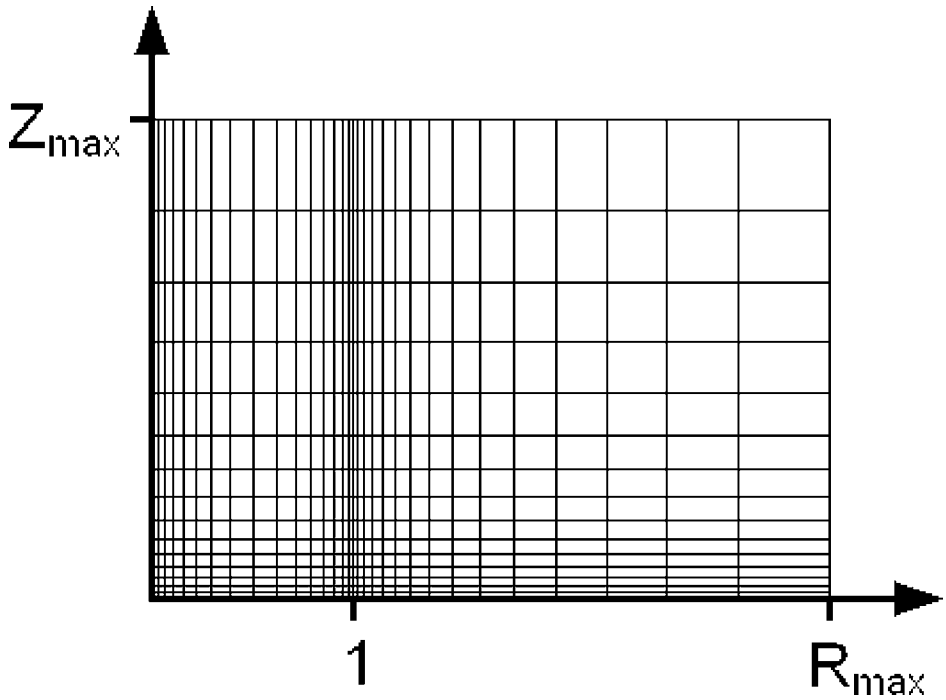


**Figure 4.** Discretized grid used in the simulations (some points have been removed for clarity).

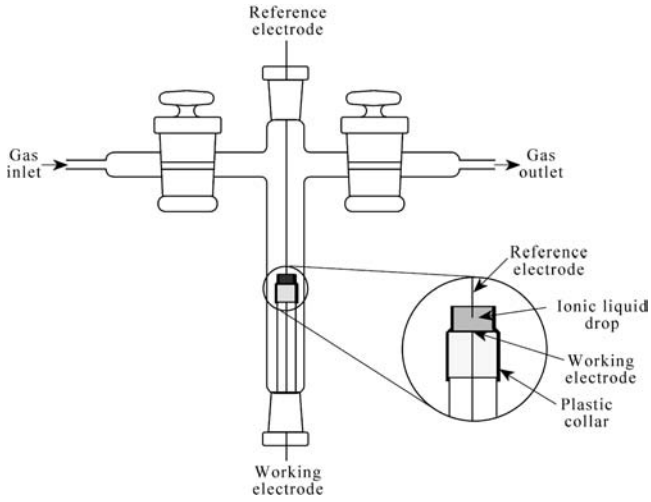


**Figure 5.** Cross section of the T-cell used to perform chronoamperometry.

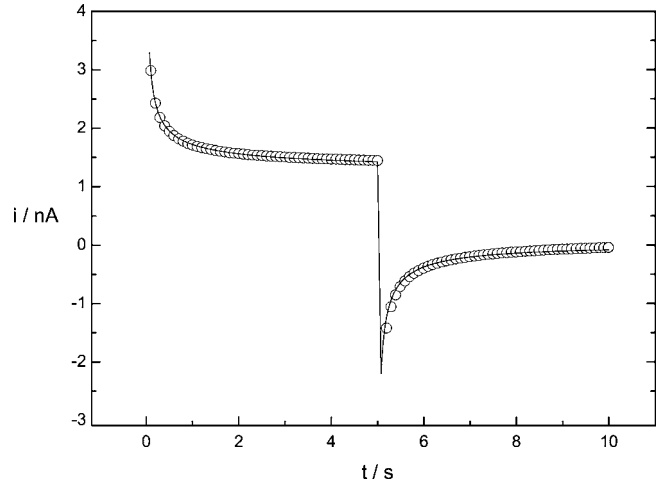


**Figure 6.** Chronoamperometric fit: —, experiment; ○, simulation.

**Table 3. Fitted Data for DMPD in [$C_4$mim][$BF_4$]**

| parameter | experimental value |
|---|---|
| $\alpha_{DMPD/DMPD^+}$ | (0.5 ± 0.1) |
| $\alpha_{DMPD^+/DMPD^{2+}}$ | (0.5 ± 0.1) |
| $c_{DMPD}$ | (19.5 ± 1.0) mM |
| $E^{\Theta}_{f,\,DMPD/DMPD^+}$ | (0.205 ± 0.01 V vs Pt |
| $E^{\Theta}_{f,\,DMPD^+/DMPD^{2+}}$ | (0.745 ± 0.01) V vs Pt |
| $k^0_{DMPD/DMPD^+}$ | ≥ 0.01 cm·s$^{-1}$ |
| $k^0_{DMPD^+/DMPD^{2+}}$ | (0.001 ± 0.002) cm·s$^{-1}$ |
| $D_{DMPD}$ | (2.0 ± 0.1)·10$^{-7}$ cm$^2$·s$^{-1}$ |
| $D_{DMPD^+}$ | (1.1 ± 1)·10$^{-7}$ cm$^2$·s$^{-1}$ |
| $D_{DMPD^{2+}}$ | (7 ± 0.1)·10$^{-8}$ cm$^2$·s$^{-1}$ |
| $k_{comp}$ | (250 ± 150) dm$^3$·mol$^{-1}$·s$^{-1}$ |
| $\Delta G^{\Theta}_{comp}$ | −52.1 kJ·mol$^{-1}$ |

respectively, to the oxidation of DMPD to $DMPD^+$ and $DMPD^{2+}$. Both electron transfers are chemically reversible as indicated by the presence of two back peaks. The reliability of the fitting procedure was ensured by fitting the voltammograms over a wide range of scan rates (two orders of magnitude). The fitted voltammograms are shown in Figure 7 and the corresponding data quoted in Table 3.

The onset of electrochemical reversibility occurs in RTILs at much lower values of the electrochemical rate constant compared to other nonaqueous solvents. For example, in a classic paper by Amatore et al.,[29] electrochemical rate constants as high as 4 cm·s$^{-1}$ could be distinguished voltammetrically in acetonitrile. The reason for this discrepancy lies in the high viscosity of ionic liquid solvents (e.g., $\mu_{[C_{4mim}][BF_4]} = 112$ mPa·s at 25 °C[30]) compared to other nonaqueous solvents (e.g., $\mu_{acetonitrile} = 34$ mPa·s at 25 °C[31]). Mass transport is more likely to be rate-limiting in solvents of greater viscosity. The rate constant for the first electron transfer ($DMPD - e^- \rightleftharpoons DMPD^+$) is electrochemically reversible on the voltammetric time scale ($k^0_{DMPD/DMPD^+} \geq 0.01$ cm·s$^{-1}$), while the second ($DMPD^+ - e^- \rightleftharpoons DMPD^{2+}$) is quasi-reversible ($k^0_{DMPD^+/DMPD^{2+}} = (0.001 \pm 0.002)$ cm·s$^{-1}$).

The comproportionation of DMPD and $DMPD^{2+}$ to form $DMPD^+$ is thermodynamically downhill. Using eq 5 and the data in Table 3, $\Delta G^{\Theta} = -52.1$ kJ·mol$^{-1}$. However, from the Table 3, comproportionation is slow on the voltammetric time

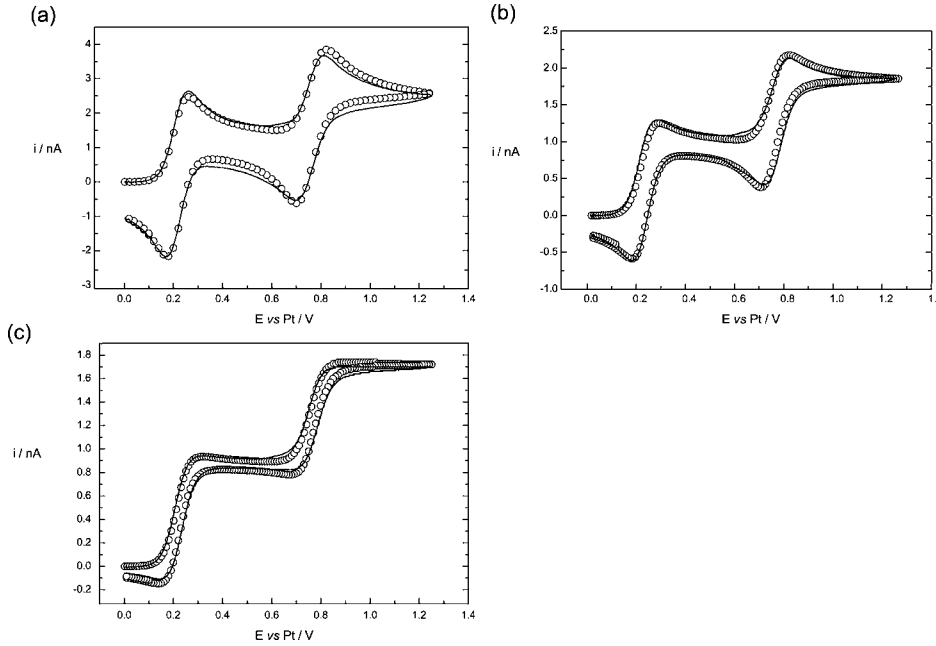


**Figure 7.** Voltammetric fits: —, experiment; ○, simulation ($k_{comp}$ = 250 dm$^3$·mol$^{-1}$·s$^{-1}$). (a) 1000 mV·s$^{-1}$, (b) 100 mV·s$^{-1}$, and (c) 10 mV·s$^{-1}$.

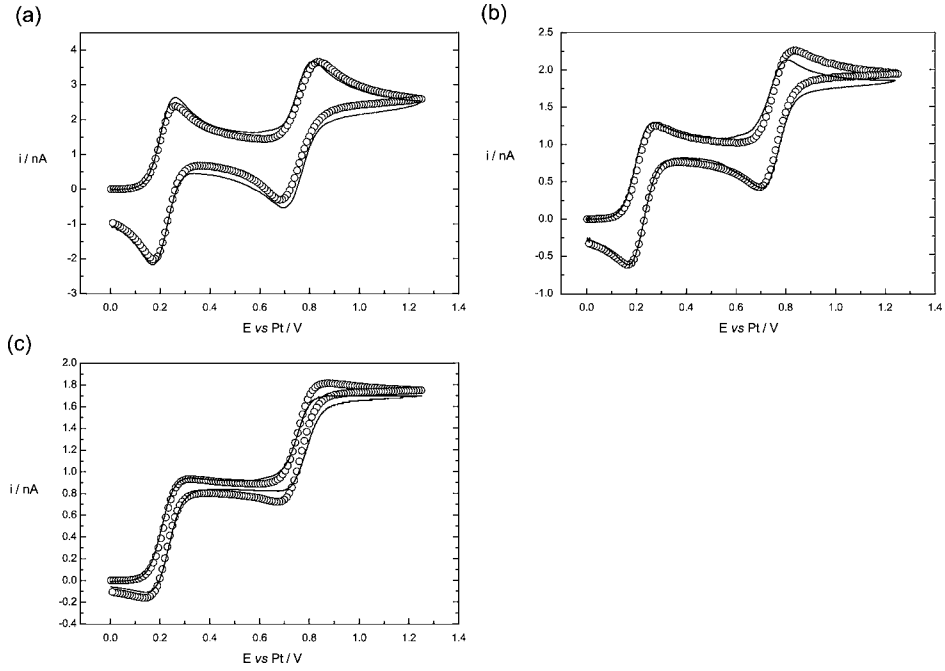


**Figure 8.** Voltammetric fits: —, experiment; ○, simulation ($k_{comp}$ = 0 dm$^3$·mol$^{-1}$·s$^{-1}$). (a) 1000 mV·s$^{-1}$, (b) 100 mV·s$^{-1}$, and (c) 10 mV· s$^{-1}$.

scale ($k_{comp}$ = 250 dm$^3$·mol$^{-1}$·s$^{-1}$). When DMPD is oxidized, the lone electron pair on each nitrogen atom makes an increased contribution to the resonance within the aromatic ring: the double bond character of each of the C−N bonds increases. The rearrangement energy for the electron transfer is substantial and leads to a small value of the rate constant as laid out in Marcus theory.[32,33]

In a recent paper[7] it was shown that, in the limit of electrochemical reversibility, the presence of diffusionally controlled comproportionation can be discerned only at high scan rates when the diffusion coefficients of the species ($D_{DMPD}$, $D_{DMPD^+}$, and $D_{DMPD^{2+}}$) are significantly different such that $D_{DMPD^+}/D_{DMPD} > 1.5$ and $D_{DMPD^{2+}}/D_{DMPD} > 1.5$ or $D_{DMPD^+}/D_{DMPD} < 0.75$ and $D_{DMPD^{2+}}/D_{DMPD} < 0.75$. It is important to note that this conclusion refers to a comparison between $k_{comp}$ = 0 dm$^3$·mol$^{-1}$·s$^{-1}$ and *diffusion control*. For an arbitrary value of $k_{comp}$ the aforementioned conditions for the observation of comproportionation are neither necessary nor sufficient. Figure 8 shows a comparison between the experimental voltammograms at a range of scan rates and the simulated transients corresponding to the data in Table 3 with $k_{comp}$ = 0 dm$^3$·mol$^{-1}$·s$^{-1}$. It is clear that, for the present system, the occurrence of comproportionation *can* be identified voltammetrically, and the discrepancy between $k_{comp}$ = 0 dm$^3$·mol$^{-1}$·s$^{-1}$ and $k_{comp}$ = 250 dm$^3$·mol$^{-1}$·s$^{-1}$ increases with decreasing scan rate. At low scan rates a steady-state voltammetric response is obtained, while at high scan rates comproportionation is outrun on the voltammetric time scale. Therefore, in each case, the presence of comproportionation cannot be discerned from the voltammetry. For DMPD in [$C_4$mim][$BF_4$], the effect of comproportionation is not expected to be apparent in the limit of very low scan rates.

## 4. Conclusion

In this paper, simulation studies have been used to show that comproportionation, in which DMPD reacts homogeneously with $DMPD^+$ ($DMPD + DMPD^{2+} \rightleftharpoons 2DMPD^+$), can be discerned for the two-electron oxidation of DMPD in the ionic liquid $[C_4mim][BF_4]$. In addition, the kinetic and thermodynamic parameters of the reaction were elucidated by means of double potential step chronoamperometry and cyclic voltammetry.

## Literature Cited


(1) Wang, Y.; Sun, Y.; Yu, L.; Zeng, Z. Preparation of room temperature ionic liquids (RTILs) 1-butyl-3-methylimidazolium tetrafluoroborate and their applications in organic synthesis. *Shenyang Yaoke Daxue Xuebao* **2006**, *23*, 432–434.

(2) Mallakpour, S.; Kolahdoozan, M. Room temperature ionic liquids as replacements for organic solvents: direct preparation of wholly aromatic polyamides containing phthalimide and S-valine moieties. *Polym. J. (Tokyo, Jpn.)* **2008**, *40*, 513–519.

(3) Silvester, D. S.; Compton, R. G. Electrochemistry in room temperature ionic liquids: a review and some possible applications. *Z. Phys. Chem.* **2006**, *220*, 1247–1274.

(4) Ignat'ev, N. V.; Welz-Biermann, U.; Kucheryna, A.; Bissky, G.; Willner, H. New ionic liquids with tris(perfluoroalkyl)trifluorophosphate (FAP) anions. *J. Fluorine Chem.* **2005**, *126*, 1150–1159.

(5) Camper, D.; Bara, J. E.; Gin, D. L.; Noble, R. D. Room-Temperature Ionic Liquid-Amine Solutions: Tunable Solvents for Efficient and Reversible Capture of $CO_2$. *Ind. Eng. Chem. Res.* **2008**, *47*, 8496–8498.

(6) Zhu, S.; Chen, R.; Wu, Y.; Chen, Q.; Zhang, X.; Yu, Z. A mini-review on greenness of ionic liquids. *Chem. Biochem. Eng. Q.* **2009**, *23*, 207–211.

(7) Belding, S. R.; Baron, R.; Dickinson, E. J. F.; Compton, R. G. Modeling Diffusion Effects for a Stepwise Two-Electron Reduction Process at a Microelectrode: Study of the Reduction of para-Quaterphenyl in Tetrahydrofuran and Inference of Fast Comproportionation of the Dianion with the Neutral Parent Molecule. *J. Phys. Chem. C* **2009**, *113*, 16042–16050.

(8) Barnes, A. S.; Rogers, E. I.; Streeter, I.; Aldous, L.; Hardacre, C.; Compton, R. G. Extraction of Electrode Kinetic Parameters from Microdisc Voltammetric Data Measured under Transport Conditions Intermediate between Steady-State Convergent and Transient Linear Diffusion as Typically Applies to Room Temperature Ionic Liquids. *J. Phys. Chem. B* **2008**, *112*, 7560–7565.

(9) Andrieux, C. P.; Savéant, J. M. Electro-Oxidation of 1,2-ene-diamines. *J. Electroanal. Chem.* **1970**, *28*, 339–348.

(10) Amatore, C.; Bonhomme, F.; Bruneel, J.-L.; Servant, L.; Thouin, L. Mapping dynamic concentration profiles with micrometric resolution near an active microscopic surface by confocal resonance Raman microscopy. Application to diffusion near ultramicroelectrodes: first direct evidence for a conproportionation reaction. *J. Electroanal. Chem.* **2000**, *484*, 1–17.

(11) Belding, S. R.; Rogers, E. I.; Compton, R. G. Potential Step Chronoamperometry at Microdisc Electrodes: Effect of Finite Electrode Kinetics. *J. Phys. Chem. C* **2009**, *113*, 4202–4207.

(12) Evans, R. G.; Klymenko, O. V.; Price, P. D.; Davies, S. G.; Hardacre, C.; Compton, R. G. A comparative electrochemical study of diffusion in room temperature ionic liquid solvents versus acetonitrile. *ChemPhysChem* **2005**, *6*, 526–533.

(13) Paddon, C. A.; Silvester, D. S.; Bhatti, F. L.; Donohoe, T. J.; Compton, R. G. Coulometry on the voltammetric timescale: microdisk potential-step chronoamperometry in aprotic solvents reliably measures the number of electrons transferred in an electrode process simultaneously with the diffusion coefficients of the electroactive species. *Electroanalysis* **2007**, *19*, 11–22.

(14) Klymenko, O. V.; Evans, R. G.; Hardacre, C.; Svir, I. B.; Compton, R. G. Double potential step chronoamperometry at microdisk electrodes: simulating the case of unequal diffusion coefficients. *J. Electroanal. Chem.* **2004**, *571*, 211–221.

(15) Zigah, D.; Ghilane, J.; Lagrost, C.; Hapiot, P. Variations of Diffusion Coefficients of Redox Active Molecules in Room Temperature Ionic Liquids upon Electron Transfer. *J. Phys. Chem. B* **2008**, *112*, 14952–14958.

(16) Endres, F.; Zein El Abedin, S. Air and water stable ionic liquids in physical chemistry. *Phys. Chem. Chem. Phys.* **2006**, *8*, 2101–2116.

(17) Hapiot, P.; Lagrost, C. Electrochemical Reactivity in Room-Temperature Ionic Liquids. *Chem. Rev. (Washington, DC, U. S.)* **2008**, *108*, 2238–2264.

(18) Buzzeo, M. C.; Klymenko, O. V.; Wadhawan, J. D.; Hardacre, C.; Seddon, K. R.; Compton, R. G. Voltammetry of Oxygen in the Room-Temperature Ionic Liquids 1-Ethyl-3-methylimidazolium Bis((trifluoromethyl)sulfonyl)imide and Hexyltriethylammonium Bis((trifluoromethyl)sulfonyl)imide: One-Electron Reduction To Form Superoxide. Steady-State and Transient Behavior in the Same Cyclic Voltammogram Resulting from Widely Different Diffusion Coefficients of Oxygen and Superoxide. *J. Phys. Chem. A* **2003**, *107*, 8872–8878.

(19) Ghilane, J.; Lagrost, C.; Hapiot, P. Scanning electrochemical microscopy in nonusual solvents: inequality of diffusion coefficients problem. *Anal. Chem.* **2007**, *79*, 7383–7391.

(20) Britz, D. *Digital Simulation in Electrochemistry*; Springer-Verlag: New York, 2005.

(21) Heinze, J. Diffusion processes at finite (micro) disk electrodes solved by digital simulation. *J. Electroanal. Chem.* **1981**, *124*, 73–86.

(22) *Numerical Recipes: The Art of Scientific Computing*; Press, W. H., Teukolsky, S. A., Vetterling, W. T., Flannery, B. P., Eds.; Cambridge University Press: New York, 2007.

(23) Gavaghan, D. J. An exponentially expanding mesh ideally suited to the fast and efficient simulation of diffusion processes at microdisc electrodes. 1. Derivation of the mesh. *J. Electroanal. Chem.* **1998**, *456*, 1–12.

(24) Sharp, M. Determination of the charge-transfer kinetics of ferrocene at platinum and vitreous carbon electrodes by potential-step chronocoulometry. *Electrochim. Acta* **1983**, *28*, 301–308.

(25) Schroder, U.; Wadhawan, J. D.; Compton, R. G.; Marken, F.; Suarez, P. A. Z.; Consorti, C. S.; de Souza, R. F.; Dupont, J. Water-induced accelerated ion diffusion: voltammetric studies in 1-methyl-3-[2,6-(S)-dimethylocten-2-yl]imidazolium tetrafluoroborate, 1-butyl-3-methylimidazolium tetrafluoroborate and hexafluorophosphate ionic liquids. *New J. Chem.* **2000**, *24*, 1009–1015.

(26) O'Mahony, A. M.; Silvester, D. S.; Aldous, L.; Hardacre, C.; Compton, R. G. Effect of Water on the Electrochemical Window and Potential Limits of Room-Temperature Ionic Liquids. *J. Chem. Eng. Data* **2008**, *53*, 2884–2891.

(27) Evans, R. G.; Klymenko, O. V.; Saddoughi, S. A.; Hardacre, C.; Compton, R. G. Electroreduction of Oxygen in a Series of Room Temperature Ionic Liquids Composed of Group 15-Centered Cations and Anions. *J. Phys. Chem. B* **2004**, *108*, 7878–7886.

(28) Shoup, D.; Szabo, A. Chronoamperometric current at finite disk electrodes. *J. Electroanal. Chem.* **1982**, *140*, 237–245.

(29) Amatore, C.; Maisonhaute, E.; Simonneau, G. Ultrafast cyclic voltammetry: performing in the few megavolts per second range without ohmic drop. *Electrochem. Commun.* **2000**, *2*, 81–84.

(30) Okoturo, O. O.; VanderNoot, T. J. Temperature dependence of viscosity for room temperature ionic liquids. *J. Electroanal. Chem.* **2004**, *568*, 167–181.

(31) Cunningham, G. P.; Vidulich, G. A.; Kay, R. L. Several properties of acetonitrile-water, acetonitrile-methanol, and ethylene carbonate-water systems. *J. Chem. Eng. Data* **1967**, *12*, 336–337.

(32) Compton, R. G.; Banks, C. E. *Understanding Voltammetry*; World Scientific: Singapore, 2007.

(33) Marcus, R. A. The theory of oxidation-reduction reactions involving electron transfer. I. *J. Chem. Phys.* **1956**, *24*, 966–978.


Received for review September 23, 2009. Accepted October 26, 2009. We thank the following for funding: Honeywell Analytics (A.M.O'M.) and the EPSRC (S.R.B.).

JE900770B